NÖHÜ Müh. Bilim. Derg. / NOHU J. Eng. Sci., Erken Görünüm / InPress
Niğde Ömer Halisdemir Üniversitesi Mühendislik Bilimleri Dergisi
Niğde Ömer Halisdemir University Journal of Engineering Sciences
Araştırma makalesi / Research article
www.dergipark.org.tr/tr/pub/ngumuh / www.dergipark.org.tr/en/pub/ngumuh

Experimental investigation of the parameters affecting the surface roughness of materials with different thicknesses by abrasive water jetting: Polymer, composite and elastomer materials

Aşındırıcı su jeti ile farklı kalınlıklardaki malzemelerin yüzey pürüzlülüğüne etki eden parametrelerin deneysel incelenmesi: Polimer, kompozit ve elastomer malzemeler

Celalettin Baykara[1,*]

[1] *Sakarya University of Applied Sciences, Technology Faculty, Department of Mechanical Engineering, 54187, Sakarya, Türkiye*

Abstract

The surface quality of various industrial products is important for end users. For this reason, it plays an important role to obtain the desired quality of the product surface in optimum time without additional operation by applying various parameters during the production phase. In this study, it was aimed to investigate the surface quality of cast polyamide 6 (PA6 G), composite (CFRP) and ethylene propylene diene manomer rubber (EPDM) materials of different thicknesses after cutting at different feed rates in abrasive water jet (AWJ). In the experiments where a total of 99 cutting operations were carried out, the effect of material type, cutting speed and material thickness on surface quality was analysed. The test specimens were cut at low, medium and high speeds determined according to the physical properties of three different polymer, composite and elastomer based materials and the surface wear roughness was measured at three different points along the depth of cut. The results obtained were then compared with the optimum cutting speeds for different materials and thicknesses. As a result, it has been shown that the cutting speed has a significant effect on the surface quality of the surface wear and the presence of machining marks on different thicknesses and different material surfaces.

Keywords: Abrasive water jet, Polymer, Carbonfibre, Elastomer, Surface wear (roughness)

Öz

Çeşitli endüstriyel ürünlerin yüzey kalitesi son kullanıcılar yönünden önem taşımaktadır. Bu nedenle, üretim aşamasında çeşitli parametreler uygulanarak ürün yüzeyinin ilave operasyon uygulamadan uygun değer zaman içinde istenen kalitede elde edilmesi önemli rol oynamaktadır. Bu çalışmada, farklı kalınlıklarda dökme polimada 6 (PA6 G), kompozede (CFRP) ve etilen profilden dine manom er kauçuk(EPDM) malzemelerin aşındırıcı su jetinde (ASJ) farklı ilerleme hızlarında kesilmesi sonrasında malzeme kalınlığına bağlı yüzey kalitesi incelenmesi amaçlanmıştır. Toplam 99 adet kesim işleminin gerçekleştirildiği deneylerde malzeme türünün, kesme hızının ve malzeme kalınlıklarının yüzey kalitesine etkisi incelenmiştir. Polimer, kompozit ve elastomer tabanlı üç farklı malzemenin fiziksel özelliklerine göre belirlenen düşük, orta ve yüksek devirli hızlarda kesilen deney numuneleri, kesme derinliği boyunca farklı üç noktadan yüzey aşınma pürüzlüğü ölçülmüştür. Daha sonra elde dilen sonuçlar malzeme bazında ve kalınlıklarda en uygun kesme hızları karşılaştırılmıştır. Sonuç olarak, kesme hızının yüzey aşınmasının yüzey kalitesi ve farklı kalınlıklarda ve farklı malzeme yüzeylerinde işleme izlerinin varlığı üzerinde önemli bir etkiye sahip olduğu gösterilmiştir.

Anahtar kelimeler: Aşındırıcı su jeti, Polimer, Karbonfiber, Elsatomer, Yüzey aşınması (pürüzlülüğü)

1 Introduction

In response to the rapidly developing material technology, it is imperative to transform these materials into higher quality products in production systems, to process products with complex geometries with precise dimensional tolerances and to develop production technology with proactive research and development operations and new production methods to be taken against the strong competitive environment taken place by many actors in the dünya çapında market. In general terms, wear is a tribological metaphor that weakens the mechanical properties of the material by removing chips from the material [1]. However, the concept of abrasion can be used in industrial applications with different applications, such as surface roughening with chemical processes such as cataphoresis for industrial applications and in strength-enhancing preliminary preparations in bonding processes as positively [2-5]. Abrasive water jet (AWJ) abrasion of the workpiece, which is one of the non-traditional production methods, is one of the most intensively researched material cutting methods, although it is a different method. It is widely used in different industries today for cutting a wide diversity of materials such In response to the rapidly developing material technology, it is imperative to transform

* Sorumlu yazar / Corresponding author, e-posta / e-mail: cbaykara@subu.edu.tr (C. Baykara)
Geliş / Recieved: 01.12.2024 Kabul / Accepted: 18.01.2025 Yayımlanma / Published: xx.xx.20xx
doi: 10.28948/ngmuh.1594355

these materials into higher quality products in production systems, to process products with complex geometries with precise dimensional tolerances and to develop production technology with proactive research and development operations and new production methods to be taken against the strong competitive environment taken place by many actors in the global market. In general terms, wear is a tribological metaphor that weakens the mechanical properties of the material by removing chips from the material. However, the concept of abrasion can be used in industrial applications with different applications, such as surface roughening with chemical processes such as cataphoresis for industrial applications and in strength-enhancing preliminary preparations in bonding processes as positively. Abrasive water jet (AWJ) abrasion of the workpiece, which is one of the non-traditional production methods, is one of the most intensively researched material cutting methods, although it is a different method. It is widely used in different industries today for cutting a wide diversity of materials such as rubber, metal, fibreglass, wood, marble and plastics [6]. Basically, AWJ is the process in which the mass of the abrasive particles is given kinetic energy by the high water pressure of the abrasive particles and the momentum effect generated by a certain acceleration, through the nozzle, the abrasive particles hit the the workpiece surface to be processed with repeated impacts in jet form and the kinetic energy is converted into pressure energy. The interaction of water, abrasive and workpiece in the water jet process, under the constant impact of the water jet, part of the abrasive particules were sprayed onto the workpiece surface in jet form, and the launch θ angle of the jet diminished with the increase of the impact pit, and gradually water and abrasives accumulated at the bottom of the impact pit (Figure 1 a-d) [7]. The abrasive particules and accumulated water occured a cushioning effect for the subsequent jet, which absorbed part of the kinetic energy of the jet, leading to an increase in energy loss and hindering the subsequent material fracturing process [8]. Since the stress generated by the abrasive grain under the compressive force is higher than the yield stress of the workpiece, it starts to form cracks in the workpiece, which then propagate and wear the workpiece, causing material erosion (Figure 2) [7, 9-11]. AWJ has no geometrical and morphological distortion of the workpiece due to the absence of thermal deformation with low cutting forces [12-14]. Moreover, it exhibits strong cutting capabilities and can cut materials of any hardness with good cutting quality. Therefore, it is an ideal method for cutting glass and other brittle materials. It is easy to operate and suitable for machining complex structures with high machining efficiency. The end product properties produced by AWJ can be tested by analysing various parameters of performance such as depth of penetration, Kerf Taper Ratio (KTR), Material Removal Rate (MRR), surface roughness etc.[15]. Wear or roughness of surface occured by the impact of abrasive particles on the workpiece surface is one of the basic criterion to asses the quality of the cut surfaces obtained by AWJ cutting [16, 17]. Surface roughness is affected by parameters such as type and thickness of the workpiece, abrasive flow rate, abrasive type, hardness, toughness and size [18, 19].

In this research, it is aspired to investigate the speed of cutting effect on the surface wearing depending on the thickness in AWJ operation of polymer materials. Therefore, it is critically important the relationship between surface wearing belong to product and the processing parameters.

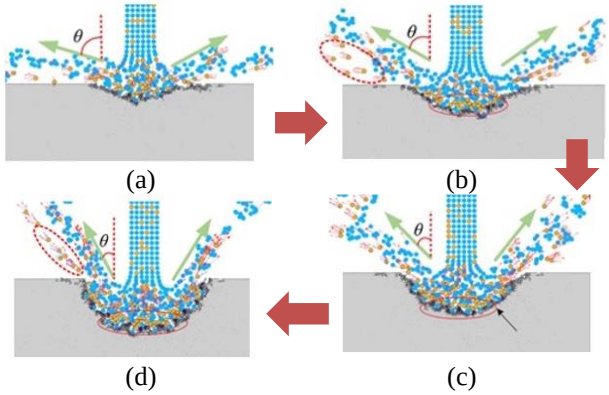

Figure 1. Machining of workpiece in abrasive water jet with respect to time [7]

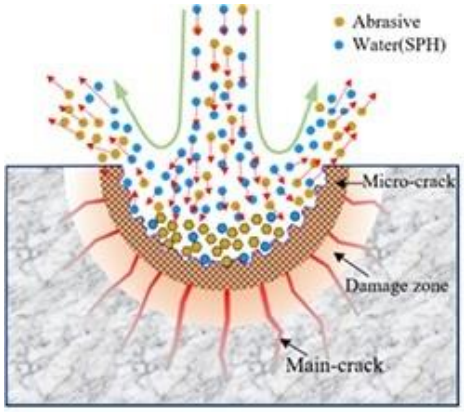

Figure 2. Chip formation on the workpiece [7]

In the manufacturing sector, manufacturing processes such as surface modification, hole drilling and cutting have been successfully applied with manufacturing methods that are unconventional from traditional methods in material cutting methods [20, 21]. Among these manufacturing methods, AWJ and Laser Beam (LB) methods have become popular in various fields of industry. The surface quality of workpieces in AWJ and laser methods is determined by various factors. In AWJ method, there is no thermal effect on the material. Water and abrasive particles erode and cut the material by erosion, whereas in the LB method, the material is exposed to a thermal load that melts and vaporises the material with high spot and high power laser beam output. Therefore, the AWJ method preserves the integrity of the material as there is no thermal degradation and no molten material residues in the cutting zone, high machining versatility and flexibility, minimum stresses, and is a more environmentally friendly production method as it does not contain a shielding gas as in the laser method. The LB

method has high repeatability, narrower kerf width and minimum material distortion rate. Surface topographies of various materials after cutting with different methods have been the focus of researchers. Krajcarz [22] tried to determine the most effective method by examining the surface roughness of metal cutting depending on the thickness of the workpiece using the parameters of abrasive mass velocity, travelling speed and depth of cut in different cutting methods: AWJ, laser beam and plasma. As a result, it was found that the AWJ method is the most suitable method in terms of surface roughness, although it is slower and more costly than other methods. Kartal et al. [23] investigated the surface roughness of 7068 alloy aluminium materials and Fico et al. [24] investigated the surface roughness of X5CrNi18-10 (1.4301) stainless steel materials after cutting at different three thicknesses at different parameters of traverse speed, depth of cut and mass flow rate in AWJ method. Theye used a feed-forward artificial neural network (ANN) to predict the surface roughness in the experimental results. By modifying the ANN input data. As a result, they showed that the AWJ method can be a tool to optimise surface roughness measurement. Zelenak et al. [25] investigated the surface topography after cutting hard materials such as titanium by AWJ and laser beam method. When the experimental results were compared, they concluded that a cleaner surface would be obtained if the AWJ method was used. Alsoufi et al. [26] investigated the effect of AWJ and laser beam method on surface roughness and microhardness of carbon steels after cutting. They found that AWJ gave better results in terms of surface roughness, while the surface hardness was almost the same. Perzel et al. [27] analysed the comparison of surface finish quality and costs of AWJ, laser beam, plasma and oxy-fuel cutting methods. They concluded that the AWJ method is slower but achieves better surface topography, and they stated that the oxy-fuel method is the cost. Dogankaya et al. [28] enhanced the effect of AWJ parameters by using particle swarm optimisation method to determine the trade-offs between surface roughness and dimensional error measurements in UHMPWPE materials. As a result, three different industrial scenarios were developed. Kahya et al. [29] investigated the surface roughness in AWJ machining of AFRP composite materials using analysis of variance and response surface methods and verified their results with ANOVA. As an alternative to AWJ method for cutting PLA materials, Kartal et al. [30] investigated to determine the most suitable cutting tool for cutting PLA materials prepared in 3D printer. As a result, they found that different diameter milling cutters were affected by the cutting process.

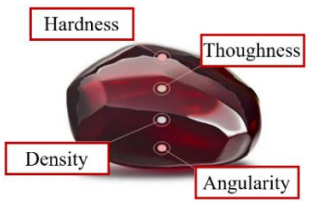

Figure 3. The properties of SiO_2 abrasive particule [31]. (Image is supplied GMA Garnet Group and reproduced with permission for this document only)

The cutting process of a material in the AWJM method is based on the principle of chip removal from the material after the abrasive particle hits the material surface. Abrasive particle properties such as hardness, toughness, density and angularity play an important role in the quality of the cutting surface (Figure 3) [31].

Type of abrasive particle: Depending on the production cost, material structure and thickness to be cut, various types of abrasive particles such as silicon dioxide (SiO_2), aluminium oxide (Al_2O_3), silicon carbide (SiC), boron carbide (B_4C), glass beads are used. Hardness of the abrasive particle: It must be higher than the hardness of the material to be machined. In industrial applications, SiO_2 and Al_2O_3 types, which are harder abrasive particles, are commonly used.

The density of the abrasive particle: An abrasive particle with a high density makes an effective impact on the surface of the material thanks to the momentum gained by the high pressure water reaching a high speed in the orifice inside the nozzle.

Toughness of the abrasive particle: When the abrasive particle hits the workpiece at high speed, it is desired that it does not disintegrate. When it disintegrates, the cutting effect is weakened.

Geometry of the abrasive particle: In order to take chips from the workpiece, the abrasive particle must have sharp corners.

Mesh size and AWJ components of the abrasive particle: Abrasive particles, whose sizes are classified as Mesh, should be selected from AWJ components in accordance with the diameter of the orifice and focusing tube. These parameters play an important role in cutting quality (Table 1).

Table 1. Surface quality parameters

Mesh no	Focusing tube diameter (mm)	Orifice diameter (mm)	Cutting quality
50, 80, 120	0.508-1.520	0.178-0.457	Excellent
60	1.070-1.270	0.305-0.356	Pro
80-120	0.508-1.070	0.178-0.356	Classic

The basic parameters of the AWJ method and the material properties used affect the surface roughness after cutting (Figure 4).

EPDM rubber material; Due to their low modulus of elasticity and viscoelastic behaviour, the processing of elastomers such as elostomer materials rubber by conventional methods causes problems such as low surface quality, These problems such as instability of dimensional, burrs and adiabatic shear band formation constitute the major obstacle for quality and economic processing. Furthermore, the machining selected method is a challenging and complex process as it is effected by the surface quality, rate of material removed, and the time required for completion. Therefore, one of the unconventional machining methods such as AWJ [32] is preferred for machining viscoelastic materials. Maurya et al. [33] researched all the unconventional processing ways that they operated to elastomers. As a result, they stated that AWJ is suitable for machining thick

elastomeric materials with improved surface quality and material removal. Hu et al. [34] studied ultra-high pressure AWJ on elastomer. As a result, they analysed the traverse speed effect (V_f) on the penetration depth during the AWJ method. They observed that at higher V_f speed, it leads to a deeper cut and the depth of cut is not maximised, while at slower V_f speed most of the energy is wasted. Cakmak et al. [35] found that the mechanical and rheological analyses of EPDM rubber with different compositions resulted in an increase in breaking stress and elongation, so the EPDM rubber obtained with the modified new formulation can be used in industry.

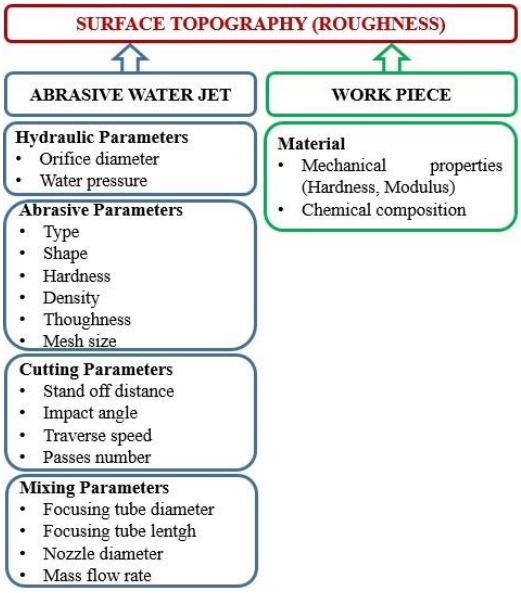

Figure 4. Parameters affecting surface quality

Carbon fibre as composite material; Li et al. [36] achieved close results in AWJ cutting of carbon fibre reinforced polymer. As a result, they observed edge rounding and a wavy slot in the upper kerf profiles, whereas, in the lower kerf profile, in addition this, they observed partial penetration, wavy edges, slits, and increased width at the endpoints of jet. Kumaran et al. [37] found that delamination of edge and deformation of corner are typical problems during AWJ cutting for carbon fibre reinforced polymer. Madhu and Balasubramaniam [38] while examining the challenges faced by fibre-reinforced polymer composites in the AWJ process, increasing the AWJ traverse speed resulted in greater stability of the nozzle. So, it obtained in a minimum ripple pattern and less surface wear. Irina et al. [39] suggested that the critical parameter to reduce KTR during AWJ machining of carbon fibre reinforced polymer hybrid composites is stand-off distance (SOD), followed by V_f. Shenglei et al. [40] investigated kerf quality in the machining of carbon fibre reinforced plastics by multiple passes of AWJ. The analysis of experimental shown that the multiple pass parameter with increased AWJ in pre-defined ranges reduced the KTR. They stated that with high AWJ multiple pass machining should generate a relatively low V_f in the first pass cutting operation and a high V_f in the second pass cutting operation to further decrease the KTR. Besides, they observed that the delamination of the lower kerf profile that occurs in the machining of carbon fibre reinforced plastics is due to the material removal mechanism. Anand et al [41] studied thin hybrid polymer composites in AWJ method to specify the significant processing parameters. They determined that the abrasive flow rate greatly make effets the machining performance resulting from V_f. Karacor et al. [42] investigated the tensile strength and stiffness characteristics of different hybrid composite structures reinforced with Jute and carbon fibres for polyester and epoxy resin. As a result, it was observed that the use of epoxy resin resulted in a stronger structure in terms of mechanical properties and a harder structure in terms of microhardness. Sükür [43] investigated the sliding friction and wear properties of carbon fibre reinforced epoxy composites with calcium carbonate ($CaCO_3$) nano-reinforcements against metallic opposing surfaces.

PA6 G as a polymer material; High heat generation is inevitable during the engineering materials machining. The energy arising from the friction between the cutting tool, the workpiece and the separation of the atomic bonds atomic in deformation fo plastic are the major causes for the increase in temperature. Materials as metal are less affected by deformation of thermal because they have a high coefficient of thermal conductivity compared to ot her materials of engineering. Nevertheless, in polymer materials, undesirable production problems such as distortion, material plastering, increasing of surface roughness, edge build-up emerge due to high temperature [44-47]. These defects can be minimised by optimising the parameters of process in the processing of polymer materials [48]. However, optimising the parameters are not enough to enhance the quality of surface because a large amount of heat is generated in machining applications because of the load and high speed. It is important to use cutting fluids to remove heat from the workpiece. Nevertheless, the negative effects of mineral or semi-synthetic cutting fluids on the human health and environment restrict their use [49]. The using of vegetable-based coolants in machining operations in their low thermo-oxidation resistance is restricted that their low tribological performance at high temperatures. Therefore, it is require to use a critic process without heat generation to enhance the machinability for polymer materials. AWJ process, in that cutting can be fulfilled without increasing the temperature, is very efficient for increasing the machinability of polymer materials and enhancing the quality of surface [50]. Kartal et al. [51] searched the optimum parameters for maximum MRR in turning and minimum roughness of surface (R_a) low density polyethylene material by statistical and experimental methods. In conclusion, they stated that the method of AWJ is an significant method for polymers of machining. By eliminating effects of thermal in AWJ machining of polymer materials, machinability can be important enhanced [52]. But, there are still significant problems associated with ergonomics and quality of surface. The roughness of surface is intensly effective in determining the materials fatigue life operating under dynamic loads. The quality of low surface in the AWJ process is based on the burst behaviour of the water jet after exit of nozzle. Because of the pressure change, the

water jet included of abrasive particules and water is dispersed on the workpiece. Due to this breakout behaviour, since the hardness and sharp form of the abrasive particles in the cutting jet are higher than the workpiece, when they hit the workpiece with high pressure, the surface quality of the material deforms and wear occurs. In addition this, the AWJ operating method generates problems as spatter and noise due to the high pressure. During high pressure AWJ, it generates unacceptable levels of noise (~110 dB) for the health of workers [53, 54]. To solve the surface quality and noise ergonomics problems, so the dispersion behaviour of the abrasive particles in the jet nozzle should be kept under control. Mindivan [55] investigated the effect of nanosized graphene particles used as fillers on the structural and thermo-mechanical properties of Polyamide 6/Graphene Nanolayer (PA6/GNP) composites. As a result, it was concluded that the thermo-mechanical properties of composites were improved thanks to their new and dominant crystal structures.

Since there are generally AWJ cutting studies focused on metal materials within the scope of the literature, in this research, it is aimed to examine the cutting processes of plastic, rubber and composite materials of different thicknesses other than metal materials at different traverse speeds in the AWJ method, which is an innovative aspect that will contribute to the literature.

2 Mathematical modelling of smoothed partical hydrodynamics (SPH) for abrasive water jet

2.1 SPH basic theory

The erosion phenomenon of abrasive particles causing roughening of the workpiece surface is analysed by repeated impacts of these particles with a water jet, whereas the investigate of the effect of a single abrasive particle can be beneficial in understanding the parameters such as particle shape, impact angle and impact velocity that are effective in material deformation and chip removal mechanisms such as cutting, cracking. Reducing the abrasion mechanism to single particle impact analysis provides applicability, numerical analysis techniques, robustness and validation of material models. Experimental research can be verified by numerical analysis with SPH method. Therefore, the wear mechanism can be explained by mathematical modelling of the abrasive particles on a single abrasive particle. SPH method, which does not have a mesh structure (without mesh), provides an advantage in the simulation of particle impacts since it does not include deformable elements in the SPH structure, as opposed to analysis methods with grid-based mesh structure encountered in large deformation problems such as mesh entanglement and element distortion [65]. The method of SPH is based upon the algorithm that distributes the fluid and abrasive particles into a series of particles that simulate the flow of the fluid by interacting with each other. The continuous phase in the SPH analysis domain is decomposed into finite particles carrying field and material variables (Figure 5) [66] shows the support field in the SPH method, when particle b is in the region Ω, which is the support field of particle a, the two particles interact and gain acceleration with respect to the equations of motion. Since each SPH particle has its own acceleration, the SPH method is suitable for deformation. Another advantage of the method of SPH lies in its conceptual simplicity and simple implementation, which facilitates the introduction of new physical quantities [57].

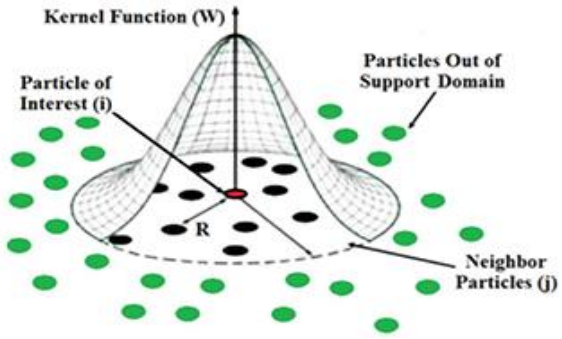

Figure 5. Support domain and smoothing function for the particle of interest, i [58]

SPH is defined by Equation (1), which expresses the integral approximation or kernel approximation of the field function f by the function ⟨f⟩ [59].

$$< f(x) >= \int_{\Omega} f(x')W(x - x', h)dx' \qquad (1)$$

where

<f(x)> is the mean value of the function f at point r in the domain Ω, the continuous field function of the particle x in the domain,

Ω: the distance of an arbitrary point from the origin

W: Correction kernel function with central peak

h: The length of the correction between the DTH particles. h indicates the size of the support area around the particle at point r.

x': The vector describing the position of all points in the domain.

The continuous integral indicate stated in Equation (1) can be transformed into discretized sums over all arbitrarily distributed particles in the domain.

This process is generally referred to as 'approximation of particle' in domain functions.

Given a correction function W for particle xi, for a number of particles N at position xi in the domain, the approximation of particle for ⟨f(x) can be stated as in Equation (2) [59].

$$< f(x_i) >= \sum_{j=1}^{N} \frac{m_i}{\rho_j} f(x_i).W(x_i - x_j, h) \qquad (2)$$

where,

m_i: Particle mass

ρ_j: Particle density

In the production operations with abrasive water jet, water can be defined as a plastic material when it hits the workpiece that is more rigid than itself. So, the pressure and volumetric strain increase are expressed by the slope of the

linear relationship between Us and Up with an equation of state (Equation (3)).

$$U_s = c_0 + sU_p \quad (3)$$

where

c_0: Mass speed of sound for pure water medium

s: Slope of linear Us-Up Hugoniot form in equation of state

Therefore, the Mie-Grüneisen equation of state (Equation (4)) can be used to describe the pressure

$$P = \frac{\rho_0 c_0^2 \eta}{(1 - s\eta)^2}\left(1 - \frac{\Gamma_0 \eta}{2}\right) + \Gamma_0 \rho_0 E_m \quad (4)$$

P: Pressure

ρ_0: reference density

$\eta = 1 - \rho_0 \rho^{-1}$ is nominal volumetric compressive stress

c_0^2: elastic bulk modulus for small nominal stresses

Γ_0: Grüneisen ratio

E_m: internal energy per unit mass

2.2 Abrasive particules and surface roughness

The abrasive particles used in the abrasive water jet are applied to the workpiece one after another, removing chips from the workpiece surface and causing erosion, and the surface becomes rough. For a good surface erosion process, the hardness, toughness, angularity and density of the abrasive particles must be at the highest level. Each abrasive grain hits the surface at high speed one after another and removes the chip (Figure 6 a-d) [60]. As a result of these grains multiplying and hitting the workpiece, roughness occurs on the surface. The surface quality obtained after the process plays a critical role in reducing the operation cost.

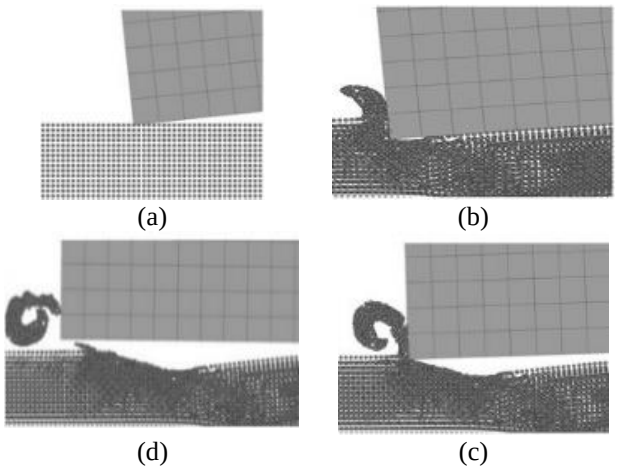

Figure 6. Simulation of chip detachment from the surface of workpiece [71]

3 Materials

Three types of ductile materials of different thicknesses were used during the experiment to investigate the quality of surface for the workpiece with abrasive grains in the AJM structure. These materials were cut by AJM method at different traverse speeds and their surface qualities were analyzed.

Cast polyamide (PA6 G) as Polymer material (Figure 7); It is an engineering polymer material produced by anionic polymerization casting process that is resistant to physical, mechanical and chemical effects such as abrasion, impact, fatigue and corrosion, as well as high dimensional stability, lighter and economical than metals due to its easy to process and low density. By changing the polymerization conditions, the material properties of PA6 G (Table 2) [61] can be modified according to specific applications, which can be improved by adding various additives, fillers, lubricants and dyes to improve the molecular structure, properties and performance [62, 63]. It is used in a diversity of industrial applications, including rotary and sliding moving parts in shafts, slides and bushings, gears etc. [64, 65].

Figure 7. PA6 G as polymer material

Table 2. Material properties of PA6 G [61]

Material Properties	Unit	Value
Density	g cm^{-3}	1.15
Tensile strength	N mm^{-2}	60-70
Yield strength	N mm^{-2}	80
Allowable mean pressure deformation 1%	N mm^{-2}	26.00
Allowable mean pressure deformation 2%	N mm^{-2}	51.00
Allowable mean pressure deformation 5%	N mm^{-2}	92.00
PV limit	MPa. mms^{-1}	0.13
Flexural strength	N mm^{-2}	140
Elongation	%	> 50
Flexural modülüs	N mm^{-2}	3200
Tensile modülüs	N mm^{-2}	3500
Friction coefficient		0.35
Ball hardness	N mm^{-2}	165
Sliding wear	µm.km^{-1}	0.10
Abrasive wear		150
Notch impact resistance	Kj m^{-2}	4-25
Elastic modulus	N mm^{-2}	3000
Hardness (shore D)	-	84
Application Temperature	℃	-40-110
Melting Temperature	℃	220
Thermal conductivity	W.Km^{-1}	0.29
Electrical strength	kV.mm^{-1}	25
Water absorption	%	6.5

PA6 chemical composition is formed by the polymerization of 6-amino hexanoic acid, a 6 carbon containing compound (Figure 8). The starting material of PA6 is ε-caprolactum. Lactum is dissolved by hydrolysis.

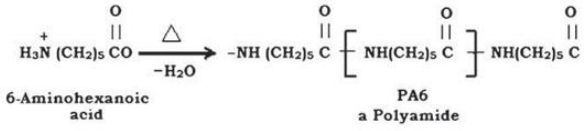

Figure 8. Chemical composition of PA 6 [63]

Carbon fiber as composite material (Figure 9); Carbon fiber is a long, thin fibrous material with about 5-10 µm. diameter and consisting mostly (93-95%) of carbon atoms. Carbon fiber (diameter 1 µm) has a tensile strength of 20 GPa, a tensile modulus of 700 GPa and a tensile modulus of 1.5×106. It has an electrical conductivity of S m^{-1} [66]. Carbon fibers are mostly formed by carbonization of materials such as rayon, polyacrylonitrile $(C_3H_3N)_n$ and pitch. Therefore, the two main components of the chemical structure of carbon fibre are carbon and polyacrylonitrile. Thousands of carbon fibers come together to form carbon fibers that are five times stronger and twice as hard as steel. It has high chemical resistance, tensile strength, hardness, weight/strength ratio. It is tolerant to extreme heat and has low thermal expansion. It is used in many industries such as aerospace, defense and automotive [67]. Carbon fibre type is classified under two groups as pitch based and Polyacrylonitrile based according to the by-products and chemical methods used. Both groups are classified in terms of strength. In this section, the mechanical properties of carbon fibre composite material from standard modulus polyacrylonite (Table 3) and low modulus pitch (Table 4) groups are shown.

Figure 9. Carbon fibre as composite material

Table 3. Mechanical properties of polyacrylonitrile based carbon fibre [67]

Properties	Unit	Value
Strain modulus	GPa	228
Strain strength	MPa	380
Elongation	%	1.6
Electrical resistivity	µΩ. cm	1650
Thermal conductivity	$W.mK^{-1}$	20
Density	$g.cm^{-3}$	1.8
Carbon content	%	95
Leaf diameter	µm	6-8

Table 4. Mechanical properties of pitch based carbon fiber [67]

Properties	Unit	Value
Strain modulus	GPa	170-241
Strain strength	MPa	1380-3100
Elongation	%	0.9
Electrical resistivity	µΩ. cm	1300
Thermal conductivity	$W.mK^{-1}$	-
Density	$g.cm^{-3}$	1.9
Carbon content	%	97
Leaf diameter	µm	11

The average chemical composition of polyacrylonitrile based carbon fibre is shown in Figure 10. Carbon fibres are materials containing more than 90% carbon and varying amounts of nitrogen, oxygen and hydrogen in their chemical structure. Their composition varies depending on oxidation conditions, temperature and time [68, 69].

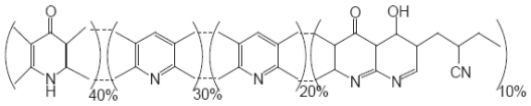

Figure 10. Representation of the chemical structure of Carbon Fibre

EPDM rubber as elastomer material (Figure 11), Elastomer is a polymeric material with both viscous properties and elastic (Table 5) and (Table 6). Elastomers are held together by longer polymeric chains driven by weak intermolecular forces (Figure 12). Once released from the applied force/tension, it recovers its original shape. When stretched, weakly held forces cause them to elongate greatly and become flexible and sticky [70, 71]. Elastomers can be used in different climatic conditions as they are resistant to temperature changes. They can maintain their form in challenging conditions by showing high resistance to impacts and chemicals. They are resistant to chemicals. In addition, their waterproof feature provides an advantage. Elastomers are used in diversity industries such as renewable energy, automobile, oil and gas, and biomedical [72, 73].

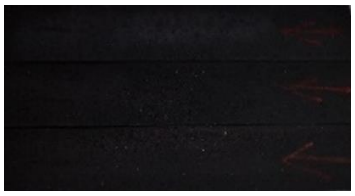

Figure 11. EPDM rubber material

Table 5. Mechanical properties of EPDM rubber [70]

Physical Properties	Unit	Value
Density	$g.cm^{-3}$	0.860
Hardness	Shore A	40-90
Ultimate tensile strength	N mm^{-2}	17.0
Ultimate tensile strain	%	195
Elongation	%	600
Glass Transition Temp.	°C	-54

Table 6. Chemical composition of EPDM rubber [70]

Fillers	Value
Antioxitant	0.5
Zinc oxide	5.0
Sterik acid	1.0
CB	30
CZ	1.0
Thiuram MS.	2.0
Sulfur	1.5

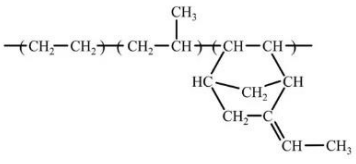

Figure 12. Representation of the chemical structure of EPDM [71]

4 Experimental studies

In this research work, cestamide, rubber, carbon fibre materials were considered during cutting with AJM during the experiment. Preliminary preparation was made with respect to the changes in the feed rate and material thickness values to be applied in their cutting. The experiments were executed in Omax 5555 abrasive water jet machine with Servotron 40.37/40.45 ultra high pressure pump, which can provide maximum 400 MPa water pressure, 37-45kW (50-60 HP) driving power, 3.8-4.6 feed rate (Figure 13). Experiments of cutting were performed at three different cutting speeds on the materials cestamide (PA6 G) (Table 7), carbon fibre (Table 8) and EPDM rubber (Table 9) with thicknesses of 10, 20, 25 and 30 mm.

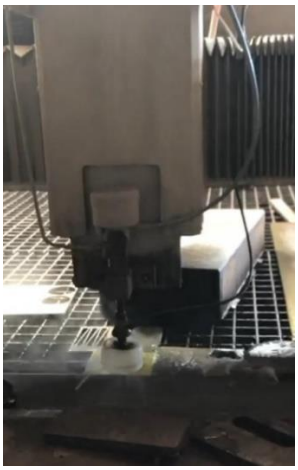

Figure 13. Representation of the cutting prosses

Table 7. PA6 G thicknesses and traverse speeds

Material Thickness (mm)	Traverse Speed (mm/min.)
10	V_1=390 V_2=500 V_3=700
15	V_1=230 V_2=300 V_3=420
20	V_1=170 V_2=220 V_3=310
30	V_1=110 V_2=150 V_3=210

Table 8. Carbon fiber thickness and traverse speeds

Material Thickness (mm)	Traverse Speed (mm/min.)
10	V_1=630 V_2=680 V_3=950
15	V_1=230 V_2=300 V_3=420
20	V_1=200 V_2=270 V_3=400
30	V_1=150 V_2=200 V_3=270

Table 9. EPDM rubber thicknesses and traverse speeds

Material Thickness (mm)	Traverse Speed (mm/min.)
10	V_1=1000 V_2=1500 V_3=2000
15	V_1=650 V_2=900 V_3=1000
20	V_1=450 V_2=600 V_3=900

Afterwards, cutting processes were performed at a constant values (Table 10), feed rates (V_1: Low rotational speed; V_2: Medium rotational speed; V_3: High rotational speed) and material thicknesses were changed. A total of 99 cutting operations were made at three different traverse speeds on the basis of three different materials with different thicknesses. The cutting speed was determined according to the thickness of the material, mechanical properties and mesh number of the abrasive particle, within the framework of AWJ fixed parameters.

Table 10. Constant parameter values in AWJ machine according to 50 HP pump

Constant parameters	Value
Orifice diameter (mm)	0.40
Focusing tube diameter (mm)	1.06
Water jet pressure (MPa)	380
Abrasive mass flow rate (gr min^{-1})	544,310
Stand off distance (mm)	2.0

The chemical composition (Table 11), physical properties (Table 12) and mesh sizes (Table 13) of silicon dioxide used as abrasive in the experiments are given as average [74].

Table 11. Average chemical composition of silicon dioxide (SiO_2) [87]

Chemical matter	Rate (%)
SiO2	35.0
Fe2O3	33.0
AlO3	23.0
MgO	7.00
MnO	1.00
CaO	1.00

Table 12. Physical properties of silicon dioxide (SiO_2) [87]

Properties	Unit	Value
Hardness	(mohs)	ca. 7.5-8.0
Abrasive size	(mesh)	80
Grain shape	-	Angular
Melting point	(°C)	1300
Spesifc gravity	(g/cm^3)	approx. 3.5-4.3
Bulk density*	(g/cm^3)	approx. 1.9-2.2

* Depending on granular size

Table 13. The mesh of Silisyum dioksit (SiO_2) for high-pressure water jet cutting [87]

Mesh	Average grain size (mm)
80	0.180-0.400
120	0.125-0.250
150	0.106-2.212
180	0.090-0.180
200	0.075-0.150
220	0.063-0.125
240	0.053-0.106
350	0.045-0.090

In the AWJ method, pure water was used as a fluid, the properties of the water used (Table 14) [7].

Table 14. Pure water parameters [7]

Density(kg m^{-3})	Velocity of Sound (m s^{-1})	Viscosity of Dynamic (Pa·s)
1000	1450	0.001

PA6 G (Table 15) and (Figure 14), carbon fibre (Table 16) and (Figure 15) and elastomer (Table 17) and (Figure 16) were cut at different traverse speeds according to their thicknesses and surface roughness values (Rz) were measured at three different points by surface profilometry in accordance with ISO 4287 standard. Then, average values of surface roughness were taken at different speeds according to PA6 G (Table 18), carbon fibre (Table 19) and elastomer (Table 20) thicknesses.

Table 15. Surface roughness values of PA6 G material at three different points at three different speeds

Sample Thickness (mm)	No. of Samples	V_1 (Low speed) Roughness values R_Z	V_2 (Medium speed) Roughness values R_Z	V_3 (High speed) Roughness values R_Z
10	1	53.80	53.80	53.80
	2	53.81	64.59	72.97
	3	59.6	68.24	66.49
15	1	51.59	52.59	63.78
	2	50.37	56.55	60.30
	3	50.49	53.78	61.28
20	1	45.40	54.07	65.21
	2	48.07	55.73	61.75
	3	46.44	49.18	58.41
30	1	48.67	55.30	68.64
	2	44.94	49.16	57.30
	3	43.28	54.47	58.61

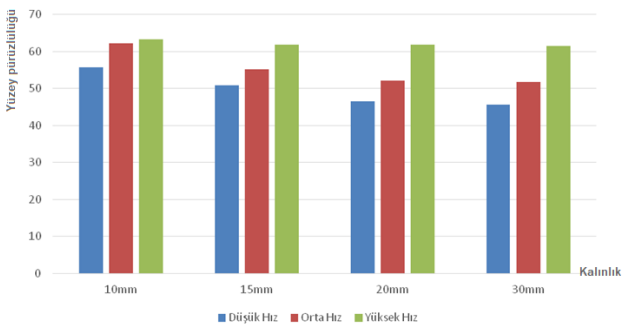

Figure 14. PA6 G Thickness-Speed-Surface Roughness (Rz)

Table 16. Surface roughness values of carbon fiber material at three different points at three different speeds

Sample Thickness (mm)	No. of Samples	V_1 (Low speed) Roughness values R_Z	V_2 (Medium speed) Roughness values R_Z	V_3 (High speed) Roughness values R_Z
10	1	64.50	53.28	67.15
	2	39.75	49.12	53.77
	3	45.00	46.93	59.70
15	1	59.92	63.02	59.34
	2	58.01	60.55	86.61
	3	45.42	61.22	75.22
20	1	76.20	72.60	79.83
	2	69.47	70.97	77.94
	3	65.00	77.76	71.02
30	1	44.77	58.65	57.56
	2	44.05	64.23	60.33
	3	48.32	49.36	79.28

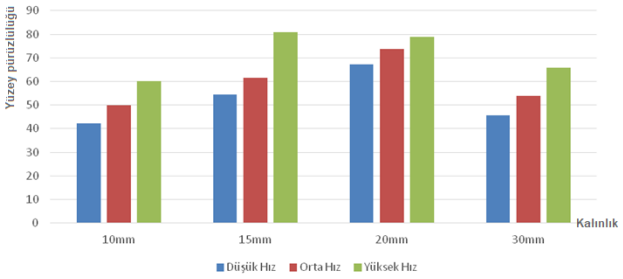

Figure 15. Carbonfibre Thickness-Speed-Surface Roughness (Rz)

Table 17. Surface roughness values of elastomer material at three different points at three different speeds

Sample Thickness (mm)	No. of Samples	V_1 (Low speed) Roughness values R_Z	V_2 (Medium speed) Roughness values R_Z	V_3 (High speed) Roughness values R_Z
10	1	52.07	50.27	56.55
	2	49.64	55.34	65.41
	3	51.97	55.48	65.45
15	1	47.10	54.22	64.66
	2	52.12	50.99	98.93
	3	52.70	58.85	62.01
20	1	70.74	88.59	87.89
	2	50.76	62.84	98.27
	3	52.08	66.36	73.24

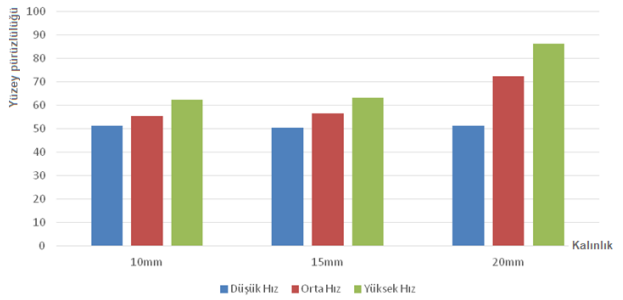

Figure 16. EPDM rubber Thickness-Speed-Surface Roughness (Rz)

Table 18. Average surface roughness values of PA6 G material at three different speeds

Material Thickness (mm)	V_1 (Low speed) Roughness values R_Z	V_2 (Medium speed) Roughness values R_Z	V_3 (High speed) Roughness values R_Z
10	55.74	62.21	63.40
15	50.82	55.16	61.79
20	46.63	52.10	61.80
30	45.63	51.80	61.52

Table 19. Average surface roughness values of carbonfibre material at three different speeds

Material Thickness (mm)	V_1 (Low speed) Roughness values R_Z	V_2 (Medium speed) Roughness values R_Z	V_3 (High speed) Roughness values R_Z
10	42.37	49.78	60.20
15	54.45	61.60	80.92
20	67.24	73.78	78.89
30	45.71	54.01	65.72

Table 20. Average surface roughness values of EPDM rubber at three different speeds

Material Thickness (mm)	V_1 (Low speed) Roughness values R_Z	V_2 (Medium speed) Roughness values R_Z	V_3 (High speed) Roughness values R_Z
10	51.23	55.41	62.47
15	50.64	56.54	63.34
20	51.42	72.60	86.47

4.1 ANOVA analysis of data and discussion of results

The following material-based results were obtained in the analysis of variance by ANOVA in MiniTab programme. The accuracy rate of the variance analysis for PA6 G is 97.8%. The P probability values of 'Material Thickness' and 'Traverse Speed' are less than 0.05. This shows that these two parameters have significant effects on surface roughness. According to this analysis, the most important parameter on surface roughness is 'Traverse Speed'. As 'Traverse Speed' increases, surface roughness increases. This effect is more pronounced in thin materials (Figure 17)

Source	DF	Seq SS	Contribution	Adj SS	Adj MS	F-Value	P-Value
Model	5	437,244	97,80%	437,244	87,449	53,26	0,0001
Linear	2	301,35	67,40%	198,918	99,459	60,57	0,0001
Material Thickness	1	71,342	15,96%	52,089	52,089	31,72	0,0013
Traverse Speed	1	230,009	51,45%	96,097	96,097	58,53	0,0003
Square	2	127,71	28,56%	32,633	16,316	9,94	0,0125
Material Thickness*Material Thickness	1	11,263	2,52%	3,189	3,189	1,94	0,2129
Traverse Speed*Traverse Speed	1	116,448	26,05%	4,333	4,333	2,64	0,1554
2-Way Interaction	1	8,183	1,83%	8,183	8,183	4,98	0,067
Material Thickness*Traverse Speed	1	8,183	1,83%	8,183	8,183	4,98	0,067
Error	6	9,852	2,20%	9,852	1,642		
Total	11	447,096	100,00%				

Figure 17. Analysis of ANOVA for PA6 G

The accuracy rate of the analysis of variance for carbon fibre is 90,72%. According to this analysis, the P probability value of both parameters is less than 0.05. Accordingly, both parameters have a significant effect on surface roughness (Figure 18).

Source	DF	Seq SS	Contribution	Adj SS	Adj MS	F-Value	P-Value
Model	5	1092,15	90,72%	1092,15	218,43	11,73	0,005
Linear	2	34,34	2,85%	158,44	79,218	4,26	0,071
Material Thickness	1	6,46	0,54%	150,61	150,61	8,09	0,029
Traverse Speed	1	27,88	2,32%	158,41	158,41	8,51	0,027
Square	2	1033,86	85,88%	317,9	158,95	8,54	0,018
Material Thickness*Material Thickness	1	977,85	81,23%	193,59	193,593	10,4	0,018
Traverse Speed*Traverse Speed	1	56,01	4,65%	0,22	0,22	0,01	0,917
2-Way Interaction	1	23,95	1,99%	23,95	23,949	1,29	0,3
Material Thickness*Traverse Speed	1	23,95	1,99%	23,95	23,949	1,29	0,3
Error	6	111,68	9,28%	111,68	18,614		
Total	11	1203,83	100,00%				

Figure 18. Analysis of ANOVA for carbon fibre

The accuracy rate of the variance analysis for the variance analysis for elastomer is 86.70%. According to this variance analysis, the effect rate of 'Material Thickness' is 32,37%. As the 'Material Thickness' increases, the surface roughness increases significantly (Figure 19).

Source	DF	Seq SS	Contribution	Adj SS	Adj MS	F-Value	P-Value
Model	5	1098,25	86,70%	1098,25	219,651	3,91	0,145
Linear	2	816,38	64,45%	546,2	273,099	4,86	0,114
Material Thickness	1	410,03	32,37%	501,62	501,62	8,93	0,058
Traverse Speed	1	406,35	32,08%	342,23	342,231	6,09	0,09
Square	2	239,51	18,91%	53,16	26,58	0,47	0,663
Material Thickness*Material Thickness	1	3,72	0,29%	32,73	32,727	0,58	0,501
Traverse Speed*Traverse Speed	1	235,79	18,61%	0,28	0,276	0	0,948
2-Way Interaction	1	42,37	3,34%	42,37	42,373	0,75	0,449
Material Thickness*Traverse Speed	1	42,37	3,34%	42,37	42,373	0,75	0,449
Error	3	168,5	13,30%	168,5	56,166		
Total	8	1266,75	100,00%				

Figure 19. Analysis of ANOVA for EPDM rubber

4.2 Confident interval (CI) analysis results

When the confidence intervals (CI) containing the group averages on the basis of material made through Minitab are examined, it is seen that there is no problem in the experimental results since PA6 G (Table 21) and (Figure 20), Carbonfibre (Table 22) and (Figure 21) and EPDM rubber (Table 23) and (Figure 22) contain 95% confidence level.

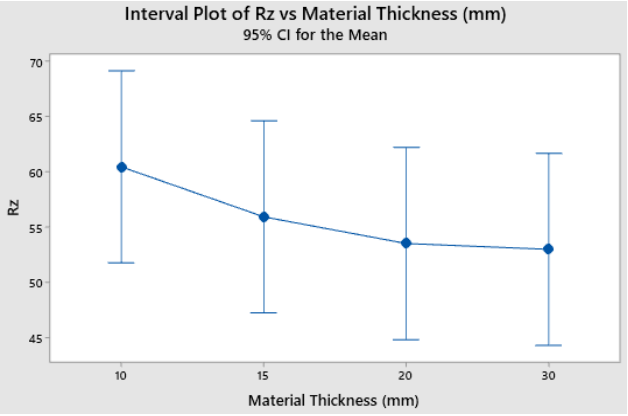

Figure 20. Confidental interval (CI) analizi for PA6 G

Table 21. Confidental Interval (CI) analizi for PA6 G

Material Thickness (mm)	N	Mean	StDev	95% CI
10	3	60.45	4.12	(51.75; 69.15)
15	3	55.92	5.52	(47.23; 64.62)
20	3	53.51	7.68	(44.81; 62.21)
30	3	52.98	8.01	(44.29; 61.68)

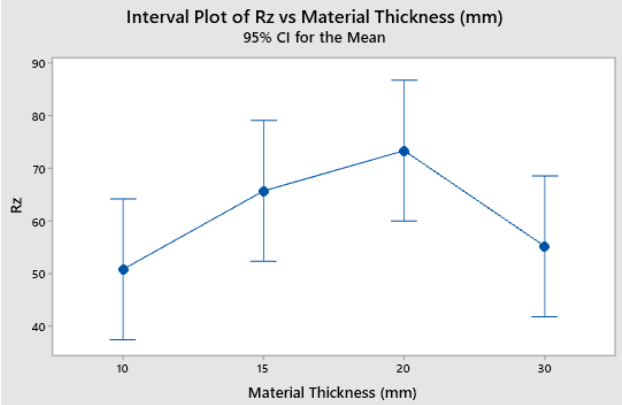

Figure 21. Confidental Interval (CI) analizi for Carbon fibre

Table 22. Confidental Interval (CI) analizi for Carbon fibre

Material Thickness (mm)	N	Mean	StDev	95% CI
10	3	50.78	8.96	(37.42; 64.15)
15	3	65.66	13.69	(52.29; 79.02)
20	3	73.30	5.84	(59.94; 86.67)
30	3	55.15	10.05	(41.78; 68.51)

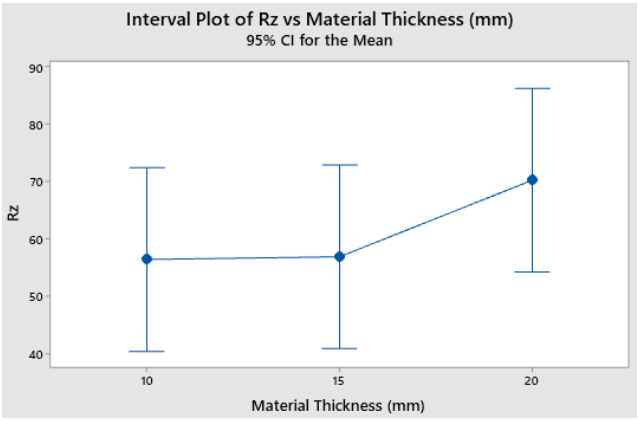

Figure 22. Confidental Interval (CI) analizi for EPDM rubber

Table 23. Confidental Interval (CI) analizi for EPDM rubber

Material Thickness (mm)	N	Mean	St.Dev	95% CI
10	3	56.37	5.68	(40.38; 72.36)
15	3	56.84	6.36	(40.85; 72.83)
20	3	70.2	17.7	(54.2; 86.2)

5 Results and discussion

In this research, the main factors affecting the surface quality due to surface roughness after cutting of non-metal such as polyamide, carbon fibre and elastomer materials of different thicknesses at different speeds in AWJ method were determined.

One of the main factors is abrasive particles. The geometrical structure, density, toughness, hardness of abrasive particless play an important role in the quality of the workpiece surface. In addition, they should not stick to the cutting surface, especially the ductile materials used in this research. For this reason, among the different types of abrasives, due to its compatibility with the material and its affordable cost Silicon dioxide (SiO_2) has been selected. Al_2O_3 can be used in harder materials. Abrasive particles are scaled in mesh units. Generally, an abrasive particle with a scale of 80 mesh is ideal for many processes. For high precision cutting, a 120 mesh abrasive will provide a better quality cut.

Another important factor is the parameters used in the AWJ machining method. In this research, different traverse speeds were used as variable parameters. It was found that the surface quality increased as the traverse speed increased. However, the parameters used in the AWJ method. Different parameters such as stand off distance, pressure, mass flow rate, focusing tube diameter and length, orifice diameter can be developed by using them as variable parameters for these materials. Among these parameters, especially the pressure of the pumped water has a very high value such as 150-620 MPa. However, using the ideal pressure 350-450 MPa ensures the long life of AJM equipment, otherwise, operating with higher pressure by using a condenser in addition to the high pressure pump shortens the service life of AJM equipment and causes more frequent failures and slows down the production process.

The last important factor is the suitability of the parameters of the material properties. In addition to the chemical and physical properties of the material, its thickness is also an important parameter. As the workpiece thickens, it increases the depth of cut and accordingly, the change in the amount of chips causes fluctuations on the surface. As a result, it causes roughness on the surface. For this reason, it is necessary to increase the kerf tapering by widening the wear zone on the workpiece surface by increasing the stand off distance from AWJ parameters, reducing the traverse speed and increasing the amount of abrasive in the water.

When AWJ method compared with cutting methods such as Laser Beam, Plasma, CNC method etc. It is understood that it is a production method with the least surface roughness. In addition, it does not cause thermal damage on the machined surfaces such as laser beam method. The absence of cutting tool costs such as CNC methods gives this method an advantage.

6 Conclusions

Although the cutting parameters and effects of various metal materials have been investigated in the AWJ method in the literature, in this study, ductile materials with different

thicknesses such as PA6 G, carbon fibre and rubber have been cut using the AWJ method under different traverse speeds in the AWJ method and an innovative research result has been added to the literature. In the experimental phase, a total of 99 cutting operations were performed. The surface quality of ductile materials with different thicknesses of traverse speed was investigated. After the cutting process, surface roughnesses were measured at three different points from the material surfaces. As a result, the effects of cutting speed and material thickness on surface quality were analysed and recommendations were made in order to shed light on future research to obtain quality surfaces in water jet cutting processes performed in industrial applications. The results obtained in this research are explained as follows.

Analysis of the effect of material type on surface quality; As a result of the abrasion mechanism that occurs with the impact effect of abrasive particles in the cutting process of the material cut with AWJ, it was observed that the surface quality decreased as the cutting speed increased in all materials used in the experiment. Therefore, roughness values increased on the material surfaces. It was determined that carbon fibre had the highest roughness value and PA6 G had the lowest roughness value in materials cut under equal conditions.

Analysis of the material thicknes effect on the quality of surface; In the PA6 G material used in the experiment, it was observed that the roughness of surface decreased as the thickness increased. In carbon fiber and rubber materials, the roughness of surface increased as the thickness increased.

Analysis of the traverse speed effect on the quality of surface; While cutting three materials with different thicknesses under equal conditions, the traverse speed was gradually increased at low, medium and high speeds. As a result, it was observed that as the speed increased, the surface roughness increased and the surface quality decreased in all materials used. It was arrived the result that the reason for this was that the materials used in the experiment did not have a rigid structure like metal materials.

Acknowledgement

The author would like to thank Prof. Dr. Ahmet DEMİRER, Mrs. Ferhande BEDIR, Mrs. Sema Nur SUEL, Mr. Çağatay YALÇIN and the personnel at Kaya Çelik Sac ve Demir Tic and Noksel Çelik Boru factories for their support in conducting the experiments during this study.

Conflict of interest

The author declares that there are no conflicts of interest.

Similarity rate (iThenticate): %12

References

[1] C. Baykara and E. Atik, The effect of surface roughness and carburized depth on wear resistance in 16MnCr5 case hardening steel. Industrial Lubrication and Tribology, 77 (1), 81-92, 2025. https://doi.org/10.1108/ILT-05-2024-0152

[2] C. Baykara, Effects of single-lap joint at different adhesive thicknesses on fatigue strength of metals with different surface coatings. Proceedings of the Institution Mechanical Engineers, Part C: Journal of Mechanical Engineering Science, 237 (17), 1-18, 2023. https://doi.org/10.1177/09544062231152995

[3] C. Baykara, I.T. Teke and A.H. Ertaş, Effects of the single-lap joint on fatigue strength of metals with different surface coatings: a numerical simulation. E3S Web of Conferences, 402, 11011, 2023. https://doi.org/10.1051/e3sconf/202340211011

[4] C. Baykara, The effect of adhesive strength on thin-walled metal surfaces coated with cataphoresis application according to adhesive thickness. 7th International Conference on Structural Adhesive Bonding 2023, Lucas F. M. da Silva and Robert D. Adams (eds.). Springer, Porto, pp.27-39. 2024

[5] C. Baykara, Farklı kimyasal yöntemlerle kaplanmış çelik plakaların farklı yapıştırma kalınlıklarda tek bindirmeli birleştirme yöntemiyle birleştirilen numunelerin yorulma analizleri sonuçlarının wöhler eğrilerinde karşılaştırılması. Afyon Kocatepe Üniversitesi Fen ve Mühendislik Bilimleri Dergisi, 24 (1), 176-188, 2024. https://doi.org/10.35414/akufemubid.1288047

[6] P. Löchner, J. Krzysztof and P. Niesłony. Investigation of the effect of cutting speed on surface quality in abrasive water jet cutting of 316L stainless steel. Procedia Engineering, 149, 276–282, 2016. https://doi.org/10.1016/j.proeng.2016.06.667

[7] Y. Hu, F. Wang, F. Jiang, L. Hu and G. Huang. Simulation analysis of damage and energy consumption of rocks during abrasive water jet impacts based on SPH-FDEM method. Powder Technology, 449, 120418, 2025. https://doi.org/10.1016/j.powtec.2024.120418

[8] F. Huang, J. Mi, D. Li, R. Wang and Z. Zhao, Comparative investigation of the damage of coal subjected to pure water jets, ice abrasive water jets and conventional abrasive water jets, Powder Technology, 394, 909–925, 2021. https://doi.org/10.1016/j.powtec.2021.08.079

[9] M. Dua, K. Zhanga, Y. Liub, L. Fenga and C. Fana, Experimental and simulation study on the influence factorsof abrasive water jet machining ductile materials. Energy Reports, 8, 11840-11857, 2022. https://doi.org/10.1016/j.egyr.2022.09.035

[10] Y. Natarajan, P.K. Murugesan, M. Mohan, and S. A. Y. A. Khan, Abrasive water jet machining process: a state of art of review. Journal of Manufacturing Processes, 49, 271–322, 2020. https://doi.org/10.1016/j.jmapro.2019.11.030

[11] A. Ibrahim and M. Papini, Controlled depth micro-abrasive waterjet milling of aluminum oxide to fabricate micro-molds containing intersecting free-standing structures. Precision Engineering, 75, 24–36, 2022. https://doi.org/10.1016/j.precisioneng.2022.01.007

[12] A. Nouhi, J. K. Spelt and M. Papini, Abrasive jet turning of glass and PMMA rods and the micro-machining of helical channels. Precision Engineering,

53, 151–62, 2018. https://doi.org/10.1016/j.precisioneng.2018.03.010
[13] F.C. Campbell, Light Weight Materials: Understanding Basics. ASM International, Cleveland, 2012.
[14] J. Zhang, C. Han and Z. Liang, Physics of failure analysis of power section assembly for positive displacement motor, Journal of Loss Prevention in the Process Industries, 44, 414-423, 2016. https://doi.org/10.1016/j.jlp.2016.10.020
[15] C. Shi, X. Wan, X. Zhu and K. Chen, A study on mechanical properties of equal wall thickness rubber bushing of positive displacement motor based on hydroge- nated nitrile butadiene rubber ageing test, Petroleum, 8 (3), 403-413, 2021. https://doi.org/10.1016/j.petlm.2021.04.008
[16] D. Begic-Hajdarevic, A. Cekic, M. Mehmedovic and A. Djelmic, Experimental study on surface roughness in abrasive water jet cutting. Procedia Engineering, 100, 394–399, 2015. https://doi.org/10.1016/j.proeng.2015.01.383
[17] Z. Ćojbašić, D. Petković, S. Shamshirband. C.W. Tong, Ch, Sudheer, P. Janković, D. Predrag, B. Nedeljko and J. Baralić. Surface roughness prediction by extreme learning machine constructed with abrasive water jet. Precision Engineering, 43, 86-92, 2015. https://doi.org/10.1016/j.precisioneng.2015.06.013
[18] K. C. Lee, S. J. Ho and S. Y. Ho, Accurate estimation of surface roughness from texture features of the surface image using an adaptive neuro-fuzzy inference system. Precision Engineering, 29, 95–100, 2005. https://doi.org/10.1016/j.precisioneng.2004.05.002
[19] A. Akkurt, M. K. Kulekci, U. Seker and F. Ercan, Effect of feed rate on surface rough- ness in abrasive water jet cutting applications. Jorunal of Materials Processing Technology, 147, 389–396, 2004. https://doi.org/10.1016/j.jmatprotec.2004.01.013
[20] R. M. Manohar, CO_2 laser beam cutting of steels: Material issues. Journal of Lasers Applications, 18, 101-12, 2006. https://doi.org/10.2351/1.2193173
[21] J. Foldyna, L. Sitek, B. Švehla, and Š. Švehla, Utilization of ultrasound to enhance high-speed water jet effects. Ultrasonics Sonochemistry, 11 (3-4), 131-137. 2004. https://doi.org/10.1016/j.ultsonch.2004.01.008
[22] D. Krajcarz, Comparison metal water jet cutting with laser and plasma cutting, Procedia Engineering, 69, 838–843, 2014. https://doi.org/10.1016/j.proeng.2014.03.061.
[23] F. Kartal and A. Kaptan. Artificial neural network and multiple regression analysis for predicting abrasive water jet cutting of Al 7068 aerospace alloy. Sigma Journal of Engineering Natural Sciences, 42 (2), 516−528, 2024 https://doi.org/10.14744/sigma.2023.00102
[24] M. Ficko, D. Begic-Hajdarevic, H.M. Cohodar, L. Berus, A. Cekic and S. Klancnik, Prediction of surface roughness of an abrasive water jet cut using an artificial neural network, Materials, 14 (11), 3108, 2021. https://doi.org/10.3390/ma14113108
[25] M. Zelenˇa´k, J. Valícek, J. Klich and P. Zˇidkova´, Comparison of surface roughness quality created by abrasive water jet and CO2 laser beam cutting, Tehnicki Vjesnik, 19 (3), 481–485, 2011.
[26] M. S. Alsoufi, D. K. Suker, A. S. Alsabban and S. Azam, Experimental study of surface roughness and micro-hardness obtained by cutting carbon steel with abrasive waterjet and laser beam technologies, American Journal of Mechanical Engineering, 4 (5), 173–181, 2016. https://doi.org/10.12691/ajme-4-5-2
[27] V. Perzel, S. Hloch, H. Tozan, M. Yagimli and P. Hreha, Comparative analysis of abrasive waterjet (AWJ) technology with selected unconventional manufacturing processes. International Journal of Physical Sciences, 6 (24), 5587–5593, 2011. https://doi.org/10.5897/IJPS11.460
[28] E. Dogankaya, M. Kahya and H. Özgür Ünver, H. Abrasive water jet machining of UHMWPE and trade-off optimization. Materials and Manufacturing Processes, 35(12), 1339–1351, 2020. https://doi.org/10.1080/10426914.2020.1772486
[29] M. Kahya E. Doğankaya O. Çaylan Z.G. Büke and H.O. Ünver, Secondary processing of aramid with AWJ and optimization with NSGA-III. Proceedings of the Institution of Mechanical Engineers, Part E: Journal of Process Mechanical Engineering, 236 (5), 2164-2175, 2022. https://doi.org/10.1177/09544089221085325
[30] F. Kartal and A. Kaptan, Experimental Determination Of The Optimum Cutting Tool For Cnc Milling Of 3D Printed Pla Parts. International Journal of 3D Printing Technologies and Digital Industry, 7 (2), 150-160, 2023. https://doi.org/10.46519/ij3dptdi.1247636
[31] GMA Garnet Pty Ltd. https://gmagarnet.com/en/americas/waterjet-garnet, Accessed 08 January 2025
[32] K. Kowsari, J. Schwartzentruber, J.K. Spelt and M. Papini, Erosive smoothing of abrasive slurry-jet micro-machined channels in glass, PMMA, and sintered ceramics: experiments and roughness model. Precision Engineering, 49, 332-343, 2017. https://doi.org/10.1016/j.precisioneng.2017.03.003
[33] P. Maurya, G.S. Vijay, K.C Raghavendra and B. Shivamurthy, Cryogenic machining of elastomers: a review. Machining Science and Technology 25 (3), 477-525, 2021. https://doi.org/10.1080/10910344.2021.1903923
[34] Y. Hu, Y. Kang, X.C. Wang, X.H. Li, X.P. Long, G.Y. Zhai and M. Huang, Mechanism and experimental investigation of ultra-high-pressure water jet on rubber cutting. International Journal of Precision Engineering and Manufacturing, 15, 1973-1978, 2014. https://doi.org/10.1007/s12541-014-0553-0
[35] N. Çakmak and Y. E. Engin, Synthesis and characterization of ethylene propylene diene monomer (EPDM) Rubber Mixture. Niğde Ömer Halisdemir Üniversitesi Mühendislik Bilimleri Dergisi, 8 (2), 1299-1306, 2019. https://doi.org/10.28948/ngumuh.479347

[36] M. Li, X. Lin, X. Yang, H. Wu and X. Meng, Study on kerf characteristics and surface integrity based on physical energy model during abrasive waterjet cutting of thick CFRP laminates. The International Journal of Advanced Manufacturing Technology, 113, 73-85, 2021. https://doi.org/10.1007/s00170-021-06590-w

[37] S. T. Kumaran, T. J. Ko, M. Uthayakumar and M. M. Islam, Prediction of surface roughness in abrasive water jet machining of CFRP composites using regression analysis. Journal of Alloys and Compounds, 724, 1037-1045, 2017. https://doi.org/10.1016/j.jallcom.2017.07.108

[38] S. Madhu and M. Balasubramanian, Challenges in abrasive jet machining of fibre-reinforced polymeric composites - a review. World Journal of Engineering, 18 (2), 251-268, 2020. https://doi.org/10.1108/wje-05-2020-0190

[39] M. M. Irina Wong, A. I. Azmi, C. C. Lee and A. F. Mansor, Kerf taper and delamination damage minimization of FRP hybrid composites under abrasive waterjet machining. The International Journal of Advanced Manufacturing Technology, 94, 1727-1744, 2018. https://doi.org/10.1007/s00170-016-9669-y

[40] X. Shenglei, W. Peng, G. Hang and S. Damien, A study of abrasive waterjet multi- pass cutting on kerf quality of carbon fibre-reinforced plastics. The International Journal of Advanced Manufacturing Technology, 105, 4527-4537, 2019. https://doi.org/10.1007/s00170-018-3177-1

[41] G. Anand, S.V. Perumal, N. Yuvaraj and K. Palanikumar, Influence of abrasive water jet machining parameters on hybrid polymer composite. Journal of the Institution Engineers (India): Series C, 102 (3), 713-722, 2021. https://doi.org/10.1007/s40032-021-00672-0

[42] B. Karacor, and M. Özcanlı, The effect of use of different types of matrix material on mechanical characteristics in jute/carbon fiber reinforced hybrid composites. Nigde Omer Halisdemir University Journal of Engineering Sciences, 11 (2), 439-448, 2022. https://doi.org/10.28948/ngumuh.1080540

[43] E.F. Şükür. Dry sliding friction and wear properties of $CACO_3$ nanoparticle filled epoxy/carbon fiber composites. Niğde Ömer Halisdemir Üniversitesi Mühendislik Bilimleri Dergisi, 9 (2), 1108-1117, 2020. https://doi.org/10.28948/ngumuh.725631

[44] H. Takeyama and N. Lijima, Machinability of glassfiber reinforced plastics and application of ultrasonic machining. CIRP Annals, 37, 93–96, 1988. https://doi.org/10.17951/pjss/2017.50.2.155

[45] K. Weinert and C. Kempmann, Cutting temperatures and their effects on the machining behaviour in drilling reinforced plastic composites. Advanced Engineering Materials, 6, 684–689, 2004. https://doi.org/10.1002/adem.200400025

[46] W. König and P. Grass, Quality definition and assessment in drilling of fibre reinforced thermosets. CIRP Annals, 38, 119–124, 1989. https://doi.org/10.1016/S0007-8506(07)62665-1

[47] W. C. Chen, Some experimental investigations in the drilling of carbon fiber- reinforced plastic (CFRP) composite laminates. International Journal of Machine Tools and Manufacture, 37, 1097–1108, 1997. https://doi.org/10.1016/S0890-6955(96)00095-8

[48] J. Kechagias, G. Petropoulos, V. Iakovakis and S. Maropoulos, An investigation of surface texture parameters during turning of a reinforced polymer composite using design of experiments and analysis. International Journal of Experimental Design and Process Optimisation, 1 (2-3), 164-167, 2009. https://doi.org/10.1504/ijedpo.2009.030317

[49] L. M. Hlaváčˇ, I. M. Hlaváčˇová, L. Gembalová, J. Kalicˇinsky´, S. Fabian, J. Meˇštˇánek, J. Kmec and V. Mádr, Experimental method for the investigation of the abrasive water jet cutting quality. Journal of Materials Processing Technology, 209, 6190–6195, 2009. https://doi.org/10.1016/j.jmatprotec.2009.04.011

[50] C. Ma and R. T. Deam, A correlation for predicting the kerf profile from abrasive water jet cutting. Experimental Thermal and Fluid Science, 30, 337–343, 2006. https://doi.org/10.1016/j.expthermflusci.2005.08.003

[51] F. Kartal, M. H. Çetin, H. Gökkaya and Z. Yerlikaya, Optimization of abrasive water jet turning parameters for machining of low density polyethylene material based on experimental design method. International Polymer Processing, 29, 535–544, 2014. https://doi.org/10.3139/217.2925

[52] F. Kartal and Z. Yerlikaya, Investigation of surface roughness and MRR for engineering polymers with the abrasive water jet turning process. International Polymer Processing, 31, 336–345, 2016. https://doi.org/10.3139/217.3185

[53] D. K. Kalla, B. Zhang, R. Asmatulu and P. S. Dhanasekaran, Current research trends in abrasive waterjet machining of fiber reinforced composites. Material Science Forum, 713, 37–42, 2012.https://doi.org/10.4028/www.scientific.net/MSF.713.37

[54] A. Radvanská, T. Ergic´, Zˇ. Ivandic´, S. Hloch, J. Valicek and J. Mullerova, Technical possibilities of noise reduction in material cutting by abrasive water-jet. Strojarstvo, 51, 347–354, 2009.

[55] F. Mindivan, Poliamid 6/Grafen nano tabakalı (PA6/GNP) kompozitlerin termo-mekanik özelliklerinin karekterizasyonu. Niğde Ömer Halisdemir Üniversitesi Mühendislik Bilimleri Dergisi, 7 (1), 443-450. 2018. https://doi.org/10.28948/ngumuh.368631

[56] M. Takaffoli and M. Papini, Finite element analysis of single impacts of angular particles on ductile targets, Wear, 267, 144–151, 2009. https://doi.org/10.1016/j.wear.2008.10.004

[57] M. Bagheri, M. Masoud and M. Riazi, A review of smoothed particle hydrodynamics, Computational Particle Mechanics, 11(3), 1163-1219, 2023. https://doi.org/10.1007/s40571-023-00679-7

[58] Z. Mao, G.R. Liu and X. Dong. A comprehensive study on the parameters setting in smoothed particle hydrodynamics (SPH) method applied to hydrodynamics problems. Computers and Geotechnics, 92, 77-95, 2017. https://doi.org/10.1016/j.compgeo.2017.07.024
[59] G.R. Liu and M.B. Liu, Smoothed particle hydrodynamics: a mesh- free particle method. World Scientific, Singapore, 2003.
[60] M. Takaffoli and M. Papini. Material deformation and removal due to single particle impacts on ductile materials using smoothed particle hydrodynamics. Wear, 274-275, 50–59, 2012. https://doi.org/10.1016/j.wear.2011.08.012
[61] TechPlasty data sheet. https://www.techplasty.com/node/232/pdf, Accessed 08 January 2025
[62] Mega Polimer. https://megapolimer.com/dokum-polyamid-pa6g/, Accessed 03 November 2024
[63] Hakan Metal. https://www.hakanmetal.com.tr/urunler/pa-6-g-dokum-polyamid-kestamit, Accessed 03 November 2024.
[64] Aydınlar Makine-Metal San. Ve Tic. Ltd. Şti. https://aydinlarmakinametal.com.tr/urunler/muhendislik-plastikleri/cast-polyamid-pa6-g/, Accessed 03 November 2024.
[65] S. Satheeskumar and G. Kanagaraj. Experimental investigation on tribological behaviours of PA6, PA6-reinforced Al2O3and PA6-reinforced graphite polymer composites. Bulletin of Materials Science, 39(6), 1467–1481, 2016. https://doi.org/10.1007/s12034-016-1296-6
[66] A. Kausar and R. Taherian. Electrical Conductivity in Polymer Composite Filled With Carbon Microfillers. Electrical Conductivity in Polymer-Based Composites. William Andrew, Norwich, pp.41-72, 2019.
[67] Avdeso drone. https://avdesodrone.com/karbon-fiber-nedir-havaciliktaki-onemi-nelerdir/, Accessed 03 November 2024.
[68] Morgan, P. Carbon Fiber and Their Composites, CRC Press, Boca Raton, 2005.
[69] S. M. Saufi and A. F. Ismail, Development and characterization of polyacrylonitrile (PAN) based carbon hallow fiber membrane, Songklanakarin Journal of Science and Technology, 24, 843-854, 2002.
[70] J. Parameswaranpillai, C. D. Midhun Dominic, S. Mavinkere Rangappa, S. Siengchin and T. Ozbakkaloglu, Introduction to Elastombers, Elastomer Blends and Composites, pp.1-9, 2022.
[71] P. Jagadeesh, S. Mavinkere Rangappa, S. Siengchin, M. Puttegowda, S.M.K. Thiagamani, G. Rajeshkumar, M. Hemath Kumar, O.P. Oladijo, V. Fiore and M. Moure Cuadrado, Sustainable recycling technologies for thermoplastic polymers and their composites: a review of the state of the art. Polymer Composites, 43 (9), 5831-5862, 2022. https://doi.org/10.1002/pc.27000
[72] J. Karger-Kocsis, A. Mousa, Z. Major and N. Békési. Dry friction and sliding wear of EPDM rubbers against steel as a function of carbon black content. Wear, 264 (3-4), 359–367, 2008. https://doi.org/10.1016/j.wear.2007.03.021
[73] B. Zirnstein, D. Schulze and B. Schartel, Mechanical and fire properties of multicomponent flame retardant EPDM rubbers using aluminum trihydroxide, ammonium polyphosphate, and polyaniline. Materials, 12 (12), 1932, 2019. https://doi.org/10.3390/ma12121932
[74] Kuhmichel abrassive GmbH. Technique data sheet. https://www.kuhmichel.com/en/products/garnet-sand/, Accessed 10 January 2025.